Sensors & Actuators: B. Chemical 425 (2025) 136976

Contents lists available at ScienceDirect

Sensors and Actuators: B. Chemical

journal homepage: www.elsevier.com/locate/snb

# Naked-eye detection of *Legionella pneumophila* using smart fluorogenic polymers prepared as hydrophilic films, coatings, and electrospun nanofibers

Ana Arnaiz [a,*], Marta Guembe-García [a], Mario Martínez [b], Miriam Trigo-López [a], Edurne González [b], Issei Otsuka [c], Saúl Vallejos [a,*]

[a] Departamento de Química, Facultad de Ciencias, Universidad de Burgos, Plaza Misael Bañuelos s/n, Burgos 09001, Spain
[b] POLYMAT, University of the Basque Country UPV/EHU, Centro Joxe Mari Korta, Avenida de Tolosa 72, Donostia-San Sebastian 20018, Spain
[c] Univ. Grenoble Alpes, CNRS, CERMAV, Grenoble 38000, France

ARTICLE INFO

*Keywords:*
Polyacrylic films
Linear polymer
Electrospun nanofibers
Fluorescence
Legionella
Smart material
Polymeric sensors

ABSTRACT

*Legionella pneumophila* is a significant public health threat, responsible for severe diseases such as Legionnaires' disease. Traditional detection methods are often labour-intensive, time-consuming, and require sophisticated equipment. This study introduces smart fluorogenic polymeric materials for the naked-eye detection of *L. pneumophila* via protease activity. These materials, prepared as hydrophilic films, cellulose-coated linear copolymers, and electrospun nanofibers, operate on an OFF/ON FRET system, emitting fluorescence under UV light upon interaction with *L. pneumophila* proteases. Characterisation confirmed the successful immobilisation of the peptide substrate and its response to proteases. The sensors showed moderate to high sensitivity and specificity, with detection limits of $2.91 \times 10^5$, $3.64 \times 10^5$, and $4.04 \times 10^5$ CFUs/mL for the film, copolymer, and nanofiber formats, respectively. Cross-reactivity tests identified only *Pseudomonas aeruginosa* as an interferent. This novel approach offers rapid, simple, and cost-effective *L. pneumophila* detection with visible results under UV light, suitable for clinical and environmental samples. It highlights the potential for broader pathogen detection applications.

## 1. Introduction

*Legionella pneumophila*, a gram-negative pathogenic bacterium, is a significant threat to public health. Responsible for Legionnaires' disease, a severe form of pneumonia, and Pontiac fever, a milder, flu-like illness [1], this pathogen has been a crucial subject of study since its identification in 1976 following an outbreak in Philadelphia. It thrives in natural and artificial water environments, such as cooling towers, hot tubs, and plumbing systems [2], and its ability to persist in biofilms and survive intracellularly within amoebae contributes to its pathogenicity [3,4]. As an opportunistic pathogen, Legionella poses a significant public health risk, particularly for more susceptible populations such as older adults, smokers, or individuals with compromised immune systems, as they may experience severe complications during infection [5]. Human infection primarily occurs through inhaling aerosolised water droplets contaminated with the bacterium. Once infection occurs, *L. pneumophila* can grow and replicate within the alveolar cells of the lungs, causing symptoms such as muscle aches, gastrointestinal discomfort, high fever, and inflammation of the bronchi and alveoli [6].

More than 60 species of Legionella are known, several of which are associated with human infections [7]. However, the most clinically significant species is *L. pneumophila*, with serogroup 1 responsible for over 80 % of the identified cases of legionellosis in Europe. Furthermore, the EU/EEA in 2021 recorded its highest annual notification rate of Legionnaires' disease at 2.4 cases per 100,000 population, with significant variation across countries. Italy, France, Spain, and Germany accounted for 75 % of the reported cases, primarily affecting males aged 65 and above, and most cases were community-acquired [8].

Many factors are involved in the ecology and pathogenesis of *L. pneumophila*, but protein secretion stands out for its potential as a virulence factor [9–11]. Among the proteins secreted into the extracellular medium, proteases secreted through the type II secretion system play a fundamental role in obtaining amino acids to be used as the primary carbon source by the bacterium [9,12,13]. One of the proteases

* Corresponding authors.
*E-mail addresses:* anaaa@ubu.es (A. Arnaiz), svallejos@ubu.es (S. Vallejos).

https://doi.org/10.1016/j.snb.2024.136976
Received 30 July 2024; Received in revised form 15 October 2024; Accepted 18 November 2024
Available online 20 November 2024

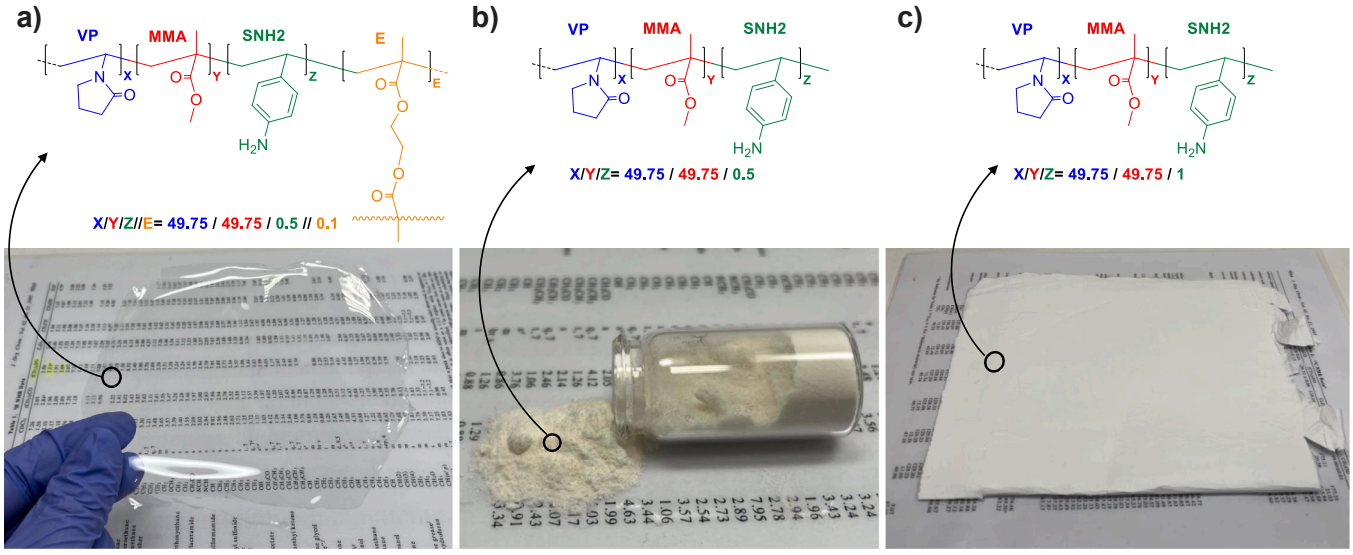


**Fig. 1.** Schematic representation and authentic images of the prepared materials: a) film; b) linear polymer; c) electrospun polymer nanofibers.

secreted in the highest proportion in the culture supernatant of *L. pneumophila* is the major secretory protein (Msp) [14–16]. This extensively studied protease consists of a zinc-metalloprotease of approximately 38 kDa, exhibiting proteolytic activity against various substrates and cytotoxic and hemolytic activity [17–20]. The potential of these proteins as virulence factors is a fascinating aspect of Legionella's pathogenicity.

Currently, several standardised and validated methods exist for Legionella detection; however, most are labour-intensive and time-consuming and require sophisticated equipment and highly qualified personnel. The most widely used is the plate culture method, according to ISO 11731:2017, which involves plating onto specific Legionella media and counting bacterial colonies and, depending on the sample type, may involve up to 14 distinct procedures [21]. On the other hand, the MPN (Most Probable Number) quantification method is developed explicitly for detecting *L. pneumophila* in water and is more straightforward than the former method [22,23]. Furthermore, the polymerase chain reaction (PCR), specifically real-time quantitative PCR (RT-qPCR), is widely utilised in the detection of Legionella in both environmental and clinical samples [24–26]. RT-qPCR is an ultra-sensitive and relatively rapid method capable of detecting minimal amounts of DNA and RNA in a sample, thereby detecting both live and dead microorganisms [21]. Finally, another technique used for Legionella detection is the Enzyme-Linked Immunosorbent Assay (ELISA), which relies on antibodies that recognise specific antigens of the bacteria. This methodology has lower sensitivity than the previous methods, but results can be obtained within a single day [27,28].

Various sensors have been developed for recognising and detecting human pathogenic bacteria, including *L. pneumophila*, based on DNA detection and quantification, and antigen-antibody interactions [29]. However, DNA sensors do not discriminate between live and dead bacteria, and those based on antigen-antibody interactions often require sample pretreatment, sophisticated equipment, and specialised personnel [30–33]. These sensors possess a broad detection range (LOD $1 \times 10^1$ to $1 \times 10^6$ CFUs/mL), relatively rapid response, and straightforward handling [33,34]. In addition, the colourimetric assays based on lateral flow assays (LFAs) were used to detect bacteria in aqueous samples such as serum, milk, or water, among others, due to their simplicity [35]. Typically, these assays employ gold nanoparticles as signal probes. However, these methods are constrained by potential sample pretreatment requirements, elevated temperatures, lengthy response times, low sensitivity, substantial sample preparation, and additional amplification steps [33].

In recent years, visual indirect methods for pathogen detection have also been developed based on the detection of biological markers secreted by these microorganisms. These markers include toxins [36], proteases [37], and even volatile organic compounds (VOCs) [38]. For instance, Mazur et al. [36] developed a paper-based sensor for the detection of listeriolysin O, a toxin secreted by *Listeria monocytogenes*, which offered a very rapid response and a meagre detection limit. However, this sensor was not evaluated directly with the pathogen nor in contaminated samples. Conversely, peptide probes and magnetic nanobeads integrated with a gold detection platform have been utilised for samples contaminated with *Staphylococcus aureus*. The advantages of this assay are its cost-effectiveness, rapid detection (within minutes), simplicity, and adaptability to other types of bacteria. Nevertheless, the colourimetric responses are not homogeneous, the stability is relatively low (6 months), and the method requires sample pretreatment and refrigeration [39]. Another example is a colourimetric sensor for *Legionellaceae* that utilises peptide probes attached to nanoparticles and deposited on a gold film. The interaction with the pathogen's proteases reacts with the substrate, revealing the underlying gold layer. The advantages of these sensors are their high specificity and ability to be used on-site [37]. However, cross-reactivity studies were conducted with a limited range of pathogens. Moreover, VOCs have been used as targets for dye-based colourimetric sensors to detect different human pathogenic bacteria in food samples, including *Escherichia coli* and *L. monocytogenes* [38]. The system uses a paper chromogenic array impregnated with different chromogenic dyes, which undergo colour changes when exposed to VOCs emitted by the pathogens. The sensor exhibits high efficiency, but the results are challenging to interpret and are integrated with machine learning algorithms, necessitating the presence of highly qualified personnel.

Our study demonstrates the feasibility of developing a polymeric material that reacts to the presence of proteases secreted by Legionella in the environment, causing a change in fluorescence through the covalent immobilisation of a peptide substrate with a FRET pair (FICT-dabcyl) in the material, and thus facilitating the naked eye detection of Legionella. A hypothetical application of such materials could be as smart labels that can be placed in high-risk areas, such as cooling towers or ventilation ducts. Although our study is primarily a proposal, this concept could enable the detection of Legionella at a glance, using only a UV lamp and eliminating the need for any analytical procedures. We recognise that this idea could lead to various final products, which is why we have explored different supporting materials: a film, linear copolymer-coated cellulose paper, and electrospun fibres. These

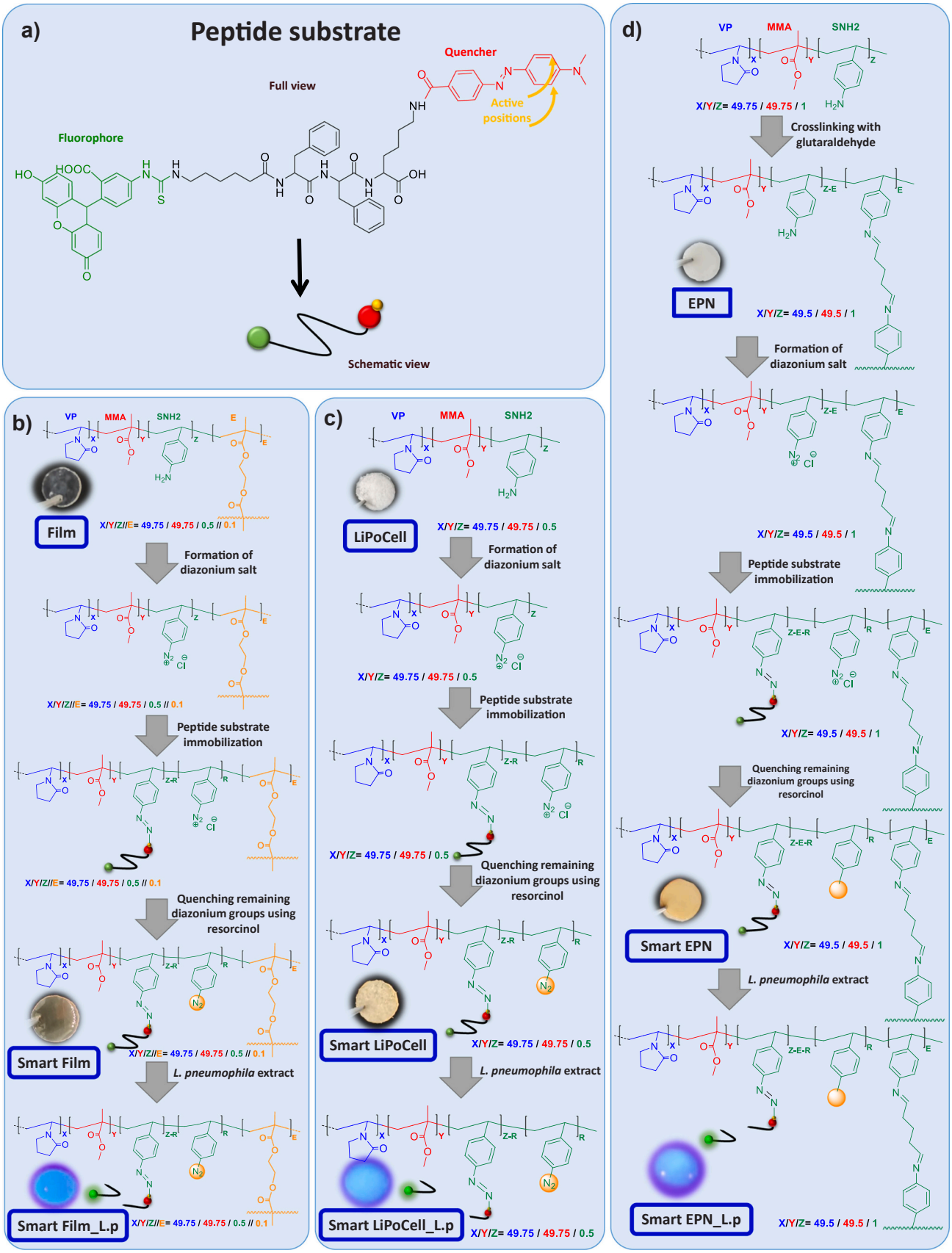


**Fig. 2.** Outline of the smart materials preparation process. a) Peptide substrate structure; b) Development of the smart materials: Film to Smart Film_L.p; c) Development of the smart materials: LiPoCell to Smart LiPoCell_L.p; d) Development of the smart materials: EPN to Smart EPN_L.p. L.p refers to *Legionella pneumophila*, meaning that these materials have already been in contact with the extract of *L. pneumophila*.

materials were tested and compared for their efficiency and properties in the detection of *L. pneumophila* through the activity of its secreted proteases.

## 2. Experimental

Materials, instrumentation, and general methods (such as material's thermal properties determination, infrared spectroscopy experiments, water swelling percentage (WSP), RAMAN spectra, inductively coupled plasma mass spectrometry, powder X-ray diffraction, electrospinning experiments, sodium dodecyl sulfate polyacrylamide gel electrophoresis, bacterial strains and inoculum preparation, etc.) are provided in the Supplementary Information (SI-Section S1).

### 2.1. Design and synthesis of the materials

For this work, three types of materials were designed (Fig. 1): a dense film, a linear polymer for cellulose filter paper coating (LiPoCell), and electrospun nanofibers (EPN). All materials were synthesised by thermally initiated bulk radical polymerisation, with a very similar composition based on three commercial monomers: *N*-vinyl-2-pyrrolidone (VP), methyl methacrylate (MMA), and 4-aminostyrene ($SNH_2$). VP contributes hydrophilicity to the material, while MMA adds hydrophobicity. Their combination produces a material with gel behaviour but with film properties. Additionally, $SNH_2$ serves as a functional point or anchoring site for sensory motifs added to the material post-polymerization (Fig. 1).

#### 2.1.1. Films

A formulation consisting of 49.75 mol% VP, 49.75 mol% MMA, and 0.5 mol% SNH2 was utilised for the films. Additionally, 0.1 mol% of ethylene glycol dimethacrylate (E) was added as the crosslinking agent to improve workability. Crosslinked materials allow working with organic solvents without being dissolved in them. Bulk polymerisation was carried out at 60 °C using 1 wt% AIBN, serving as a thermal initiator for radicals, within a silanised glass mould with a thickness of 100 μm under an oxygen-depleted atmosphere overnight (Fig. 1a). After polymerisation, the film underwent a washing process involving three steps: water (4 times for 15 min each), acetone (4 times for 15 min each), and water again. The transition from water to acetone was done gradually.

#### 2.1.2. LiPoCell

The monomer ratio was the same as that used for the film, although no crosslinker was added in this case. This allows the polymers to be redissolved after synthesis, facilitating the coating process on paper. The polymerisation was conducted at 60 °C overnight using DMF as a solvent, with a monomer concentration of 2 M and an AIBN concentration of 0.1 M. The solution was precipitated ten times its diethyl ether volume, and the solid copolymer was purified using a Soxhlet apparatus with diethyl ether as solvent (Fig. 1b).

Finally, the copolymer was dissolved in acetonitrile at a final concentration of 50 mg/mL, then 10 μL drops were applied twice (2 × 10 μL) onto the surface of a filter paper disc (6 mm diameter, 28 $mm^2$) and incubated at 60 °C for 10 min to allow solvent evaporation.

#### 2.1.3. Electrospun nanofibers

In this case, the polymer formulation was slightly modified to include twice the amount of $SNH_2$, resulting in a concentration of 1 mol%. Consequently, the mol% of VP and MMA was recalculated to 49.5 mol% for each monomer. The polymerisation process was identical to that of the film (without solvent, using a silanised glass mould with 100 μm thickness), once again excluding the crosslinker, as electrospinning of nanofibers also requires linear polymers soluble in the appropriate solvent. The bulk polymerisation process ensures the attainment of high molecular weights, which are recommended for obtaining high-quality electrospun nanofibers. The polymer was dissolved in DMF, precipitated in ten times its volume of diethyl ether, and purified using a Soxhlet apparatus with diethyl ether as the solvent.

A 15 % by-weight polymer solution was prepared using DMF as the solvent for the spinning process. The nanofibers were obtained and collected using a Spinbox by Bioinicia (Fig. 1c). The grounded rotating collector, made of stainless steel, was positioned 17 cm from the needle tips. The applied voltage was 17 kV, and the flow rate was 2.5 mL/h. Fibers were obtained using a five-needle multi-emitter. All experiments were conducted in a controlled environment, with the electrospinning chamber's temperature and relative humidity (R.H.) ranging from 23 to 25 °C and 48–54 %, respectively. Information regarding the molecular weight and the SEM images of the electrospun nanofibers can be found in Figure S1 (SI-Section S2).

Finally, the fibres undergo a crosslinking treatment with glutaraldehyde vapours for 1 h at 60 °C to enhance their physical properties and manageability.

### 2.2. Inclusion of receptors for Legionella detection. Preparation of the smart materials

#### 2.2.1. Smart film

The peptide substrate for Legionella proteases (Fig. 2a) was immobilised following the protocol previously developed for enzyme immobilisation [40] (more information about its characterisation in SI-Section S3, Figures S2 and S3). In the first step, benzene diazonium salts were generated on the amino groups provided by the $SNH_2$ monomer. Ten film discs (6 mm diameter) were dipped in 11 mL of an aqueous solution containing 10 mL of distilled water, 1 mL of HCl (37 %), and 50 mg of sodium nitrite for 1 h at room temperature. After this, the discs were washed three times with distilled water. In the second step, the substrate was immobilised by forming diazo bonds. Each disc was dipped in 500 μL of peptide aqueous solution (50 μM) at room temperature overnight. The discs were then washed thoroughly with distilled water five times. In the third step, the non-reacted benzene diazonium groups were quenched with resorcinol by dipping each disc in 500 μL of resorcinol aqueous solution (45 mM) for 1 h at room temperature. Finally, the discs were exhaustively washed every 10 min five times to obtain the smart polymers prepared as films (Fig. 2b).

Negative and positive control materials were prepared as described below. The negative controls were prepared similarly but omitted step 2 (immobilisation of the peptide substrate). The films were labelled as "Film_Resorcinol".

The positive control was actually a fluorescence reference, prepared by performing step 1 on the films and immersing each disc in 500 μL of a 50 μM aqueous solution of fluorescein. The films were labelled as "Fluorescence reference."

#### 2.2.2. Smart LiPoCell

The methodology previously described by Arnaiz et al. [41] was used to prepare the LiPoCell smart material. The procedure for obtaining and labelling the smart materials, negative controls, and a fluorescence reference is analogous to that followed for the preparation of the Smart films, but using 6 mm diameter LiPoCell discs (Fig. 2c).

#### 2.2.3. Smart electrospun nanofibers

The procedure for obtaining and labelling the smart materials, negative controls, and a fluorescence reference is analogous to that followed for preparing the Smart films but using 6 mm diameter EPN discs (Fig. 2d).

### 2.3. Legionella culture supernatant proteases

Previous studies have demonstrated that Legionella secretes a greater amount of proteases upon entering the stationary phase of its growth cycle [42]. Proteases begin to be expressed during the latency

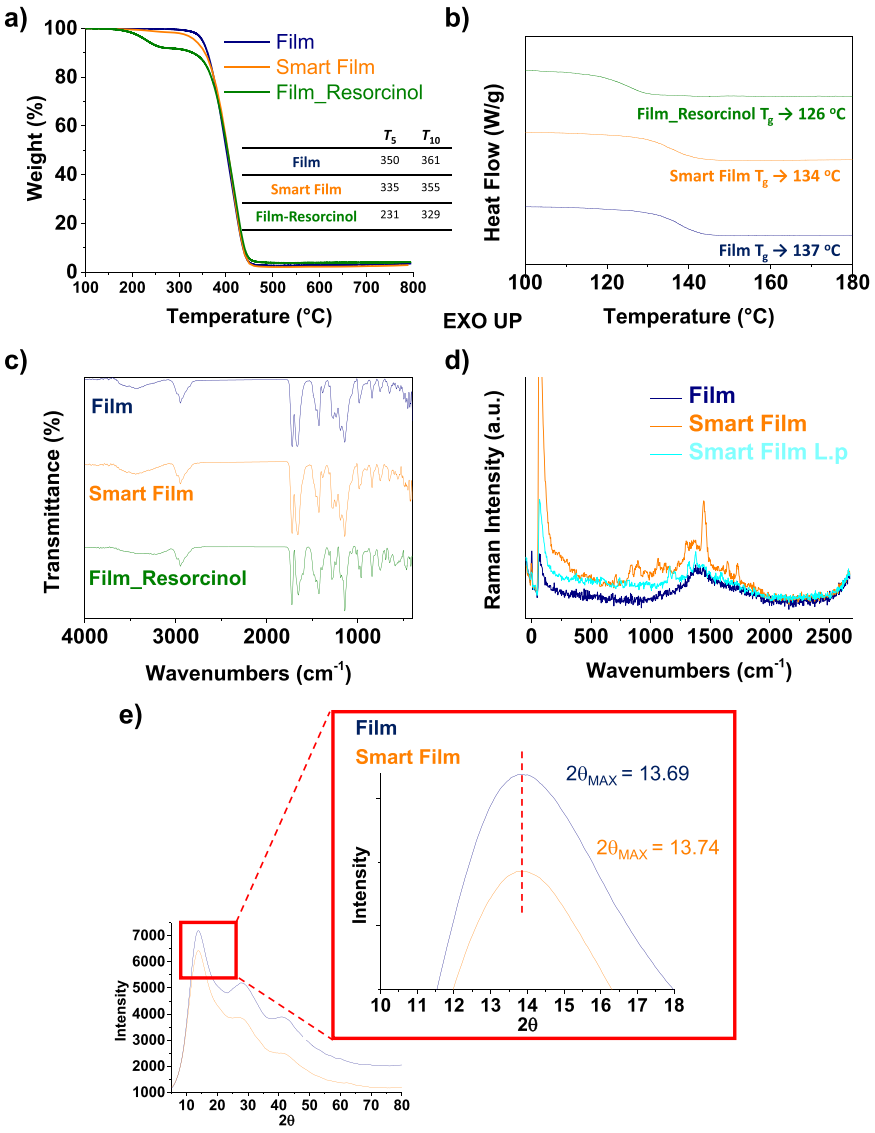


**Fig. 3.** Structure and properties of support materials. a) thermogravimetric curves of Film, Smart Film and Film_Resorcinol at 10 °C/min under a nitrogen atmosphere, displaying $T_5$ and $T_{10}$ temperatures; b) differential scanning calorimetry spectra of Film, Smart Film and Film_Resorcinol, at 20 °C·min$^{-1}$, under nitrogen atmosphere, showing the glass transition temperature ($T_g$); c) FT-IR spectrum of Film, Smart Film and Film_Resorcinol; d), RAMAN spectra Film, Smart Film; e) PXRD spectra of Film and Smart Film showing $2\theta_{MAX}$.

phase, reaching their peak expression in the early stationary phase. Naturally, this process is influenced by factors such as the growth medium, aeration, temperature, and other environmental conditions. Therefore, to obtain an extract enriched with secreted proteases from Legionella, first, liquid BYE medium was inoculated with *L. pneumophila* from a plate with BCYE medium until an O.D. of 0.3 was obtained and allowed to grow at 37 °C for 20 h at 225 rpm. Then, 0.4 mL of this initial inoculum was diluted in 20 mL of BYE liquid medium and incubated at 37 °C for 30 h at 225 rpm to reach an optical density between 2.5 and 3.5 corresponding to 3–5 × $10^9$ CFU/mL. At different growth stages, samples were taken from the culture. The optical density was measured at 600 nm, and serial dilutions were plated on BCYE medium to determine the CFUs/mL. Afterwards, the bacterial culture was pelleted by centrifugation at 3,500 *g* for 10 min, and the supernatant was filtered using a 0.22 μm nylon filter to obtain the crude protease solution.

### 2.4. Enzymatic activity of protease extracts

The activity of protease extracts was tested in microplate format. Essentially, 10 μL of protein extracts were incubated with FITC-FFK-Dabcyl substrate at a final concentration of 25 μM in the buffer 0.1 M Tris-HCl, 0.15 M NaCl, 5 mM $MgCl_2$, pH 7.5 (final reaction volume was 100 μL). Subsequently, samples were incubated at 30 °C for 1 h, and fluorescence was measured every 5 min using an excitation filter of 485/20 nm and an emission filter of 528/20 nm (Synergy HT microplate reader, BioTek®). All assays were carried out in triplicate, and blanks were used to justify spontaneous substrate breakdown.

### 2.5. Determination of the sensing systems

The activity of the smart materials was carried out in a microplate reader with 96-well plates, including a 6 mm diameter disc (Smart Film, Smart LiPoCell and Smart EPN) at the bottom of each well. The smart materials' activity was analysed using 10 μL of protease extract and 90 μL of buffer 0.1 M Tris-HCl, 0.15 M NaCl, 5 mM $MgCl_2$, pH 7.5 (final volume 100 μL). All materials were tested with blanks for spontaneous breakdown of the substrate. The assay was carried out in triplicate at 30 °C, and the fluorescence emission at 528 nm was recorded every 5 min for 1 h.

Additionally, the smart materials were tested with protease extracts

obtained at different stages of bacterial growth, following the same protease activity assay described above.

The detection limits of the three materials were estimated *in vitro* using protease cell-free supernatants from different initial growth stages of *L. pneumophila* after 1 h of incubation with the smart materials. The following equation was applied to calculate the detection limit: LOD=3.3 × SD/s, where SD is the standard deviation of the blank sample, and s is the slope of the calibration curve in the region of low CFUs/mL, respectively.

### 2.6. Determination of bacteria specificity of the smart materials

The specificity of the smart materials was evaluated against the microorganisms *Klebsiella pneumoniae*, *S. aureus*, *Salmonella enterica*, *E. coli*, and *P. aeruginosa*. Bacterial cultures were prepared as indicated in SI-Section 1. Once the bacterial cultures reached the stationary growth phase, the cell-free protease supernatants were obtained as performed for the Legionella culture (Section 2.3). Finally, the activity of the sensors was measured as described in Section 2.5.

## 3. Results and discussion

### 3.1. Design and characterisation of the polymeric materials

Legionella bacteria secrete a set of proteases into the extracellular medium during their growth and replication, which could be detected in a water sample. To efficiently prepare a sensory polymer to detect the protease in water, the polymer must contain a sufficiently high amount of a hydrophobic monomer so that the resulting copolymer is insoluble in water. However, a certain degree of hydrophilicity in the material may favour the interaction between *L. pneumophila* proteases and the substrate, so the polymer formulation must include a specific molar percentage of a hydrophilic monomer. The sensory polymers should also contain functional groups that act as anchors for immobilising the peptide substrate able to detect the protease.

The monomers' choice and proportions were based on previous studies [40,41]. The structural monomers, VP and MMA, are responsible for the material properties. Therefore, the combination of two structural monomers: one hydrophilic, VP, responsible for the swelling of the material and its compatibility with the aqueous medium, and one hydrophobic monomer, MMA, responsible for its good mechanical properties and workability, was selected. The third monomer, $SNH_2$, has a less structural and more functional role: the $NH_2$ groups of the monomer allow the anchoring of receptor units to the material, hence its low concentration in the polymer formulation.

This work studied the behaviour of a sensor system on three different supports (Film, LiPoCell, and EPN), all with an almost identical composition (Fig. 1). The binding between the fluorescent peptide substrate (based on a FRET pair) and LiPoCell was previously studied [41]. We now study and characterise the binding between the substrate and the support using the film as a model support.

The thermal properties (Fig. 3a) of the initial material, Film, show $T_5$ and $T_{10}$ values of 350 °C and 361 °C, respectively, while the material with the substrate (Smart Film) shows values of 335 °C and 355 °C. Additionally, the material with all anchoring positions blocked by resorcinol was evaluated to confirm the presence of the substrate and not just resorcinol. In this latter case, the $T_5$ and $T_{10}$ values drop to 231 °C and 329 °C, respectively. The same behaviour is observed in the $T_g$ of the material (Fig. 3b), with values of 137 °C for Film, 134 °C for Smart Film, and 126 °C in the case of Film_Resorcinol. This indicates that the substrate is anchoring, even though it does not occupy all available positions.

The FT-IR spectra (Fig. 3c) are very similar and show characteristic structures for this type of material, such as the carbonyl stretching band of the ester at 1719 $cm^{-1}$ and the -O-CH3 stretching vibrations at 1138 $cm^{-1}$, corresponding to MMA, as well as the bands at 1665 $cm^{-1}$ (carbonyl group) and at 1021 $cm^{-1}$ (C–N stretching), attributable to VP.

The Raman spectrum of Film (Fig. 3d) reflects the chemical structure of the polymer. The broad band around 1400 $cm^{-1}$ can be associated with the VP ring vibration at approximately 1420–1430 $cm^{-1}$ and the MMA $\nu_{COO\text{-}CH3}$ vibration at 1440 $cm^{-1}$. In the Raman spectrum of Smart Film, bands corresponding to the substrate can be observed and are commonly found in biological molecules. These include the $\nu_{COOH}$ vibration at 1730 $cm^{-1}$ and the $\nu_{R\text{-}CO\text{-}NHR}$ vibration at around 1650 $cm^{-1}$,

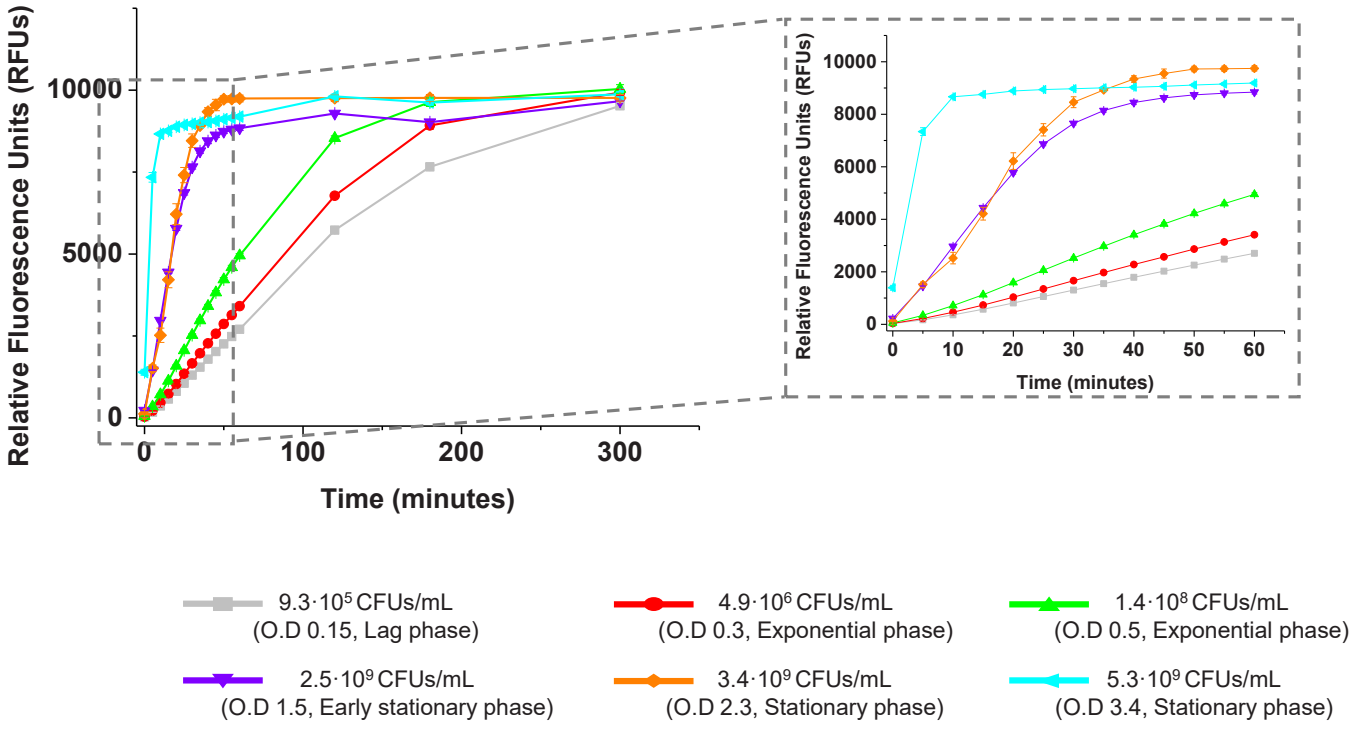


**Fig. 4.** *L. pneumophila* supernatants enzymatic activity using the FITC-Ahx-FFK-Dabcyl as substrate. Data are means ± standard error of 3 independent replicates.

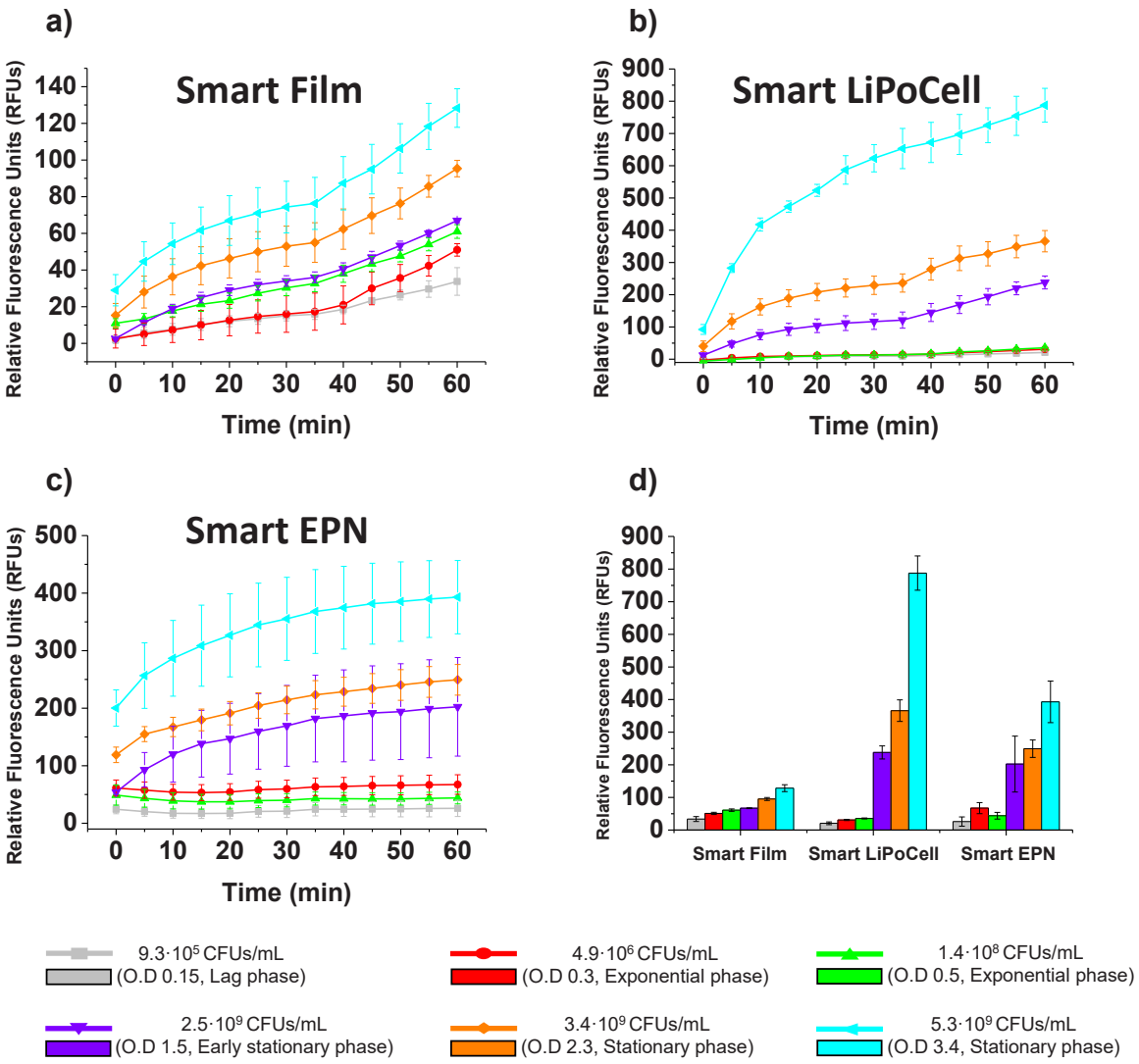


**Fig. 5.** Response of the materials Smart Film (a), Smart LiPoCell (b), and Smart EPN (c) to 10 μL of the protease extracts secreted by *L. pneumophila* at different growth phases. d) Detailed activity of the three materials after 1 h of activity assay. Data are means ± standard error of 3 independent replicates.

corresponding to the amide I band, which hydrogen bonding affects. Some of these bands disappear or lose intensity in the spectrum of Smart Film_L.p, as the interaction with the Legionella protein breaks the peptide, generating fluorescence and releasing part of the substrate. Nevertheless, the $\nu_{C\text{-}N}$ vibrations of the $RNH_2$ groups found between 1220 and 1020 $cm^{-1}$ can still be observed.

The PXRD spectrum (Fig. 3e) shows the characteristic amorphous halo of this type of material, with a maximum 2θ value of 13.69 for Film and 13.74 for Smart Film. This data allows us to calculate the interchain distance using the equation $<R> = 5/8(\lambda/\sin\theta max)$, which gives values of 8.08 and 8.05 Å, respectively. This result provides information about the orientation of the substrate inside the film after the reaction. Its linear and elongated structure makes the peptide position parallel to the polymer chain, not affecting the polymer interchain distance.

The WSP was 108 %, a common value for this combination of monomers. In this case, swelling is essential because it must be sufficient to allow interaction with biological targets without impairing the material's workability due to excessive water or solvent retention.

The chosen peptide substrate (see Fig. 2) has a fluorescein isothiocyanate derivative as its fluorophore, which contains sulfur. Quantifying sulfur serves two purposes: firstly, it demonstrates substrate binding to the material by comparing the sulfur content before (Film) and after (Smart Film) the anchoring process. Secondly, it determines the binding site; if the substrate binds via the fluorophore, the sulfur content remains unchanged between Smart Film and Smart Film_L.p. In contrast, if binding occurs through the aromatic ring containing a tertiary amine (quencher) [43], the sulfur content in Smart Film_L.p will resemble that of the starting material (Film). Therefore, a sulfur quantification study using ICP-MS was conducted to determine the substrate's binding site on the polymeric support. The values obtained for Film, Smart Film, and Smart Film_L.p. were 4.2, 13.93, and 6.48 ppm, respectively. Thus, the increase in sulfur content in Smart Film compared to Film demonstrates the substrate anchoring, whereas the low sulfur values in Smart Film_L.p, similar to Film, indicate that the substrate binds the polymer through the quencher rather than through the fluorophore.

In addition, the Supplementary Information (Figure S1, SI-Section S2) includes the characterisation of electrospun nanofibers by Gel Permeation Chromatography (GPC) and Scanning Electron Microscopy (SEM).

### 3.2. *Legionella protease extracts activity and characterisation*

Previous studies have described the role of proteins secreted by Legionella into the extracellular medium and their importance in the virulence and infection process, such as the major secretory protein (Msp) and leucine or phenylalanine peptidases [9,11,13,42].

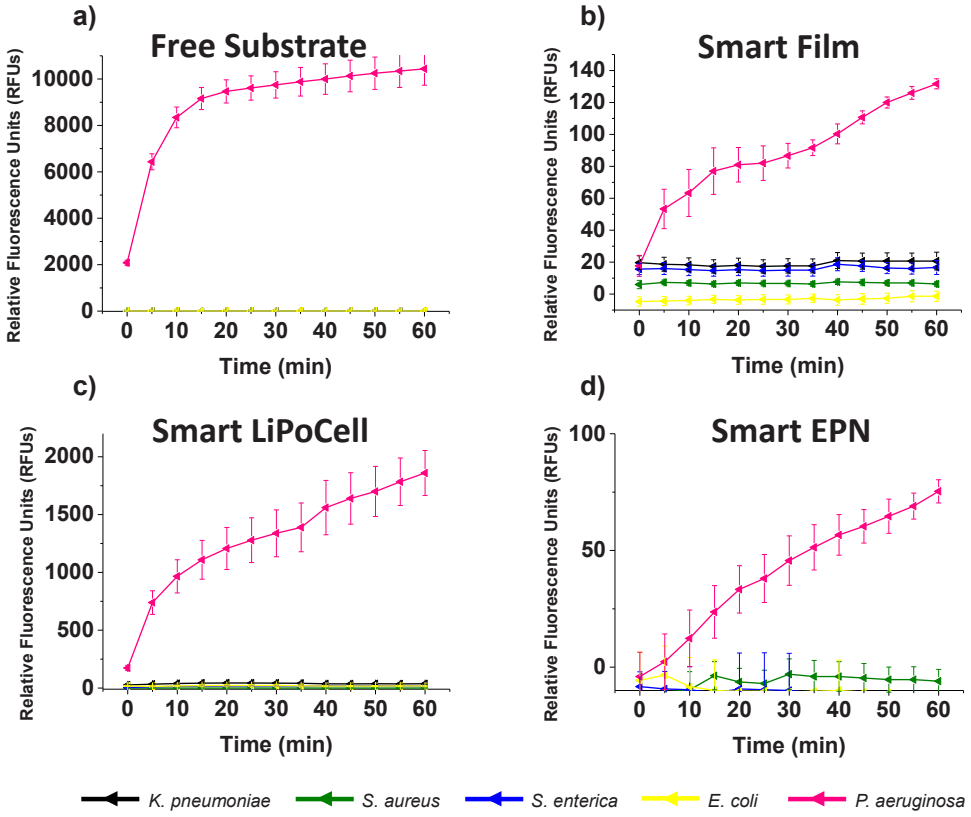


**Fig. 6.** Study of the response of the peptide substrate in solution (a) and the materials Smart Film (b), Smart LiPoCell (c), and Smart EPN (d), to 10 μL of the proteases secreted by other microorganisms grown to stationary phase. Data are means ± standard error of 3 independent replicates.

Before designing our FRET-based sensor for the proteases secreted by Legionella, we first tested the activity of this substrate in solution with different Legionella protease extracts obtained at various stages of the microorganism's growth. Figure S4 (SI-Section S4) shows the relationship between the culture's optical density (O.D) and the CFUs/mL of each extract. It is observed that the lower O.D values correspond to the lag and exponential phase of bacterial growth. Additionally, it is noted that from an O.D. of approximately 1.5, the culture enters the stationary phase, and its growth rate slows down. As shown in Fig. 4, the later the stage of Legionella growth, the more rapidly the activity with the peptide is detected. Additionally, we can observe that at the end of the assay, extracts from earlier growth stages (exponential phase-lower O.D) eventually offer the same activity for the same substrate concentration. These findings align with other researchers' findings, demonstrating that Legionella secretes increased amounts of proteases into the extracellular medium upon entering the stationary phase [42]. Consequently, the *L. pneumophila* extract exhibiting the highest activity is the one that degrades the substrate most rapidly.

These results are consistent with those observed in Figure S5 (SI-Section S4) related to the analysis of Legionella protease extracts using polyacrylamide gels. Noticeably, the proteins secreted into the medium increase as Legionella progresses in its growth phase, and the band corresponding to the major secretory protein in its active form of approximately 38 kDa (indicated by a black arrow) becomes more prominent.

### 3.3. Activity of the smart materials for Legionella detection

The polymeric materials developed in this work are based on an ON/OFF FRET system. The system is off when there are no microorganisms and, thus, no proteases in the medium to recognise the peptide. However, in the presence of Legionella-secreted proteases, the system is activated due to the proteases cleaving the substrate, generating an alert in the form of a fluorescent signal.

With this in mind, we tested the activity of three materials against Legionella extracts (Fig. 5). The smart materials' response to Legionella protease extracts varies significantly across the different formats (film, linear polymer, and fibre). During the initial growth stages of Legionella, the Smart Film (Fig. 5a) material shows the highest sensitivity and fastest detection capabilities. The Smart LiPoCell and Smart EPN (Fig. 5b-c) materials also respond effectively but with slightly less intensity and speed compared to the film when it is exposed to these protease extracts (O.D 0.1, 0.3 and 0.5). The Smart EPN (Fig. 5c) format also exhibits more significant variability in response, as evidenced by the experimental error. On the other hand, if we closely examine the response of the three materials to the various extracts of *L. pneumophila* after 1 h of incubation (Fig. 5d), it is observed that, in terms of fluorescence emission intensity, the Smart LiPoCell exhibits the highest levels, followed by the Smart EPN, and finally the Smart Film. This difference in fluorescence is primarily due to the specific characteristics of each material format. The Smart Film is the most distinct in terms of format, as shown in Fig. 2. It is a dense and transparent material, whereas the other two are fibrous and opaque. This greatly impacts the optical properties of the materials and, consequently, the fluorescence detected by the equipment. However, to the naked eye—using human vision as the detector—the fluorescence of the three materials does not appear significantly different after interaction with the proteases, as can be observed in the video in the supplementary information (SI-VIDEO).

Supplementary material related to this article can be found online at doi:10.1016/j.snb.2024.136976.

Furthermore, the LODs of the smart materials were $2.91 \times 10^5$, $3.64 \times 10^5$, and $4.04 \times 10^5$ for the Smart Film, Smart LiPoCell and Smart EPN, respectively (SI-Section S5, Figure S6). As observed, all materials present a LOD in range of $10^5$ CFUs/mL, however as expected

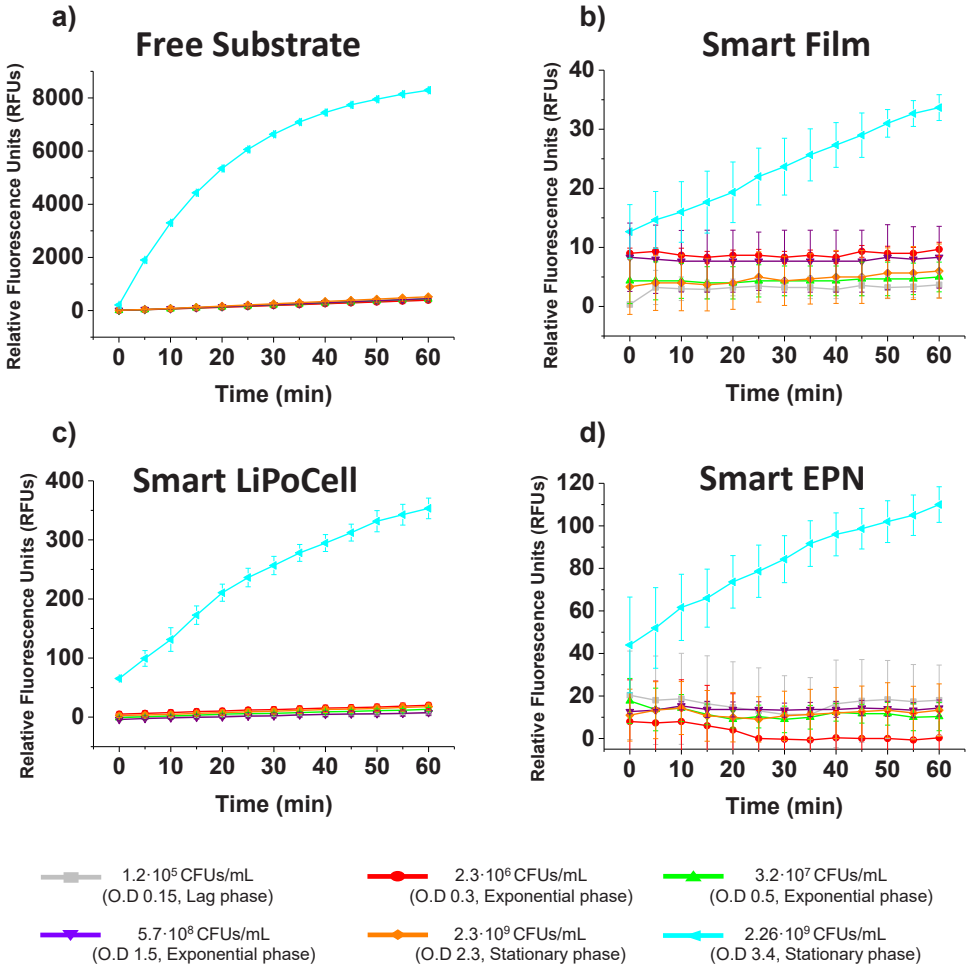


**Fig. 7.** Interference assay of the peptide substrate in solution (a) and the materials, Smart Film (b), Smart LiPoCell (c), and Smart EPN (d), to 10 μL of the protease extracts secreted by *P. aeruginosa*. Data are means ± standard error of 3 independent replicates.

by the results observed in Fig. 5, Smart Film presents the best LOD, followed by Smart LiPoCell and Smart EPN.

The video provided as supplementary information (SI-VIDEO) demonstrates the response of three smart materials to the proteases present in the Legionella extract (O.D. 3.4). This response is visibly detectable to the naked eye by simply illuminating the material under UV light.

### 3.4. Smart materials cross-reactivity

The specificity of both sensors was evaluated using extracts of proteins secreted by other microorganisms such as *S. aureus*, *K. pneumoniae*, *S. enterica*, *E. coli*, and *P. aeruginosa*. These microorganisms were chosen for their importance, as *S. aureus*, *K. pneumoniae*, and *P. aeruginosa* belong to the ESKAPE group of microorganisms (known for their high antibiotic resistance) [44,45]. *E. coli* was included in the study due to its increasing detection in various sites and its expanding antibiotic resistance [46]. *S. enterica* was included because it is one of the human pathogens commonly found in water samples, similar to *E. coli*, *P. aeruginosa*, and *L. pneumophila*. In summary, all the microorganisms selected for the cross-reactivity study are significant human pathogens that cause severe problems in the healthcare system, and some can develop and grow more quickly than others in the same environment as Legionella.

The interference of both sensors was evaluated using secreted protease extracts from all microorganisms grown to the stationary phase ($10^8$-$10^9$ CFUs/mL). First, the supernatants of the different microorganisms were evaluated for activity against the peptide in solution (Fig. 6a), and it was observed that only the protein extract of *P. aeruginosa* exhibited activity against the peptide FITC-Ahx-FFK-Dabcyl. Next, we studied the response of the three materials to these same extracts, and the results show that, once again, only *P. aeruginosa* elicited a response. The signal intensity was highest in Smart LiPoCell (Fig. 6c), followed by Smart Film and Smart EPN, which exhibited similar fluorescence intensity values (Fig. 6a, d).

All the microorganisms tested in the interference assay secrete different molecules, including proteases and other virulence factors, into the extracellular medium through different secretion systems [47]. However, the fact that only *P. aeruginosa* acts as an interferent for the three smart materials may primarily be due to specific proteases such as elastase A, elastase B, and alkaline protease, which exhibit high substrate promiscuity [48–50]. These proteases likely correspond to the most prominent bands observed in Figure S7 (SI-Section S6). We delved deeper into the interference with *P. aeruginosa* and evaluated whether the peptide in solution, as well as the three materials, responded to the supernatants from different growth stages of *P. aeruginosa* (Fig. 7). The relationship between the O.D of the *P. aeruginosa* culture and the CFUs/mL of each extract was also established (Figure S8, SI-Section S7).

As observed in all cases, the extract with the highest proteolytic activity corresponds to the latest growth phase. In solution, there is also slight activity with the supernatants from earlier growth phases (Fig. 7a). However, with the smart materials, activity is only detected with the protein extract from the most advanced growth stage, with an O.D. of 3.4 (Fig. 7b-d), even in Smart Film, which is the material with lower LOD. This is likely due to *P. aeruginosa* secreting proteases into the

medium from the beginning of its growth and replication but more intensively in the late exponential phase, with a significant increase during the stationary phase [51]. Indeed, in the results obtained after electrophoresis of these extracts (Figure S9, SI-Section S6), we can only detect the presence of proteins in the extract corresponding to O.D. 3.4 (stationary phase). Although this interference with Pseudomonas may seem like a disadvantage and a loss of sensor specificity towards Legionella, it is important to note that *P. aeruginosa* is also a dangerous pathogen for human health. Since the sensor provides a rapid and straightforward fluorescent response, we can assert that there is a pathogen, either Legionella or Pseudomonas, in the analysed sample. In any case, for the detection of a species of Legionella or Pseudomonas other than *L. pneumophila* or *P. aeruginosa*, it is likely that our sensors would yield a positive response, potentially resulting in a false positive. However, from the perspective of early detection and risk prevention, a false positive is considerably less detrimental than a false negative. Consequently, hygiene and health measures can be implemented until the specific pathogen is confirmed through other techniques, such as PCR or plate culture.

## 4. Conclusions

With this study, we have designed an indirect sensor to detect *L. pneumophila* through three different formats. This is achieved via the specific recognition of a covalently anchored fluorogenic peptide substrate (based on a FRET system) in a polymeric matrix, which is recognised by specific proteases secreted by the pathogenic bacteria. Three different formats have been developed for the same sensor (Smart Film, Smart LiPoCell and Smart EPN), offering versatility, ease of use, and a naked-eye response. From the perspective of the limit of detection (LOD), the Smart Film is the most advantageous option and undoubtedly holds promise due to the low material costs. We estimate it to be 2.8 euros for a 20 mm diameter piece. The choice of format can also be adapted to the environment or the sample type. For instance, Smart Film would be recommended for use in clinical samples (such as sputum) due to its higher sensitivity. Additionally, Smart LiPoCell and Smart EPN can aid in a quick, easy, and simple initial screening for the presence of Legionella in environmental samples. These three smart materials demonstrate remarkable adaptability and simplicity in indirectly detecting pathogens. They exhibit high specificity, effectively detecting *P. aeruginosa*, a significant health risk pathogen. Currently, this is the first sensor based on the fluorescent detection of proteolytic activity for rapid use, developed in three different formats. Although we acknowledge that it is not a final product and represents only the first step in a long journey, we believe it holds significant potential. Ultimately, it could lead to the development of products such as smart labels for the visual detection of pathogens without the need for sampling or analysis with advanced equipment, such as MALDI-TOF.

## CRediT authorship contribution statement

**Marta Guembe-García:** Writing – review & editing, Writing – original draft, Methodology, Investigation. **Mario Martínez:** Writing – review & editing, Resources, Methodology, Investigation. **Miriam Trigo-López:** Writing – review & editing, Supervision, Conceptualization. **Edurne González:** Writing – review & editing, Supervision, Resources, Methodology, Investigation. **Issei Otsuka:** Writing – review & editing, Methodology, Investigation. **Saul Vallejos:** Writing – review & editing, Writing – original draft, Supervision, Resources, Project administration, Methodology, Investigation, Funding acquisition, Conceptualization. **Ana Arnaiz:** Writing – review & editing, Writing – original draft, Validation, Methodology, Investigation, Formal analysis.

## Declaration of Competing Interest

The authors declare that they have no known competing financial interests or personal relationships that could have appeared to influence the work reported in this paper.

## Acknowledgements

We gratefully acknowledge the financial support provided by all funders. The financial support provided by Fondo Europeo de Desarrollo Regional-European Regional Development Fund (FEDER, ERDF) and Regional Government of Castilla y León -Consejería de Educación, Junta de Castilla y León- (BU025P23) is gratefully acknowledged. This work was supported by the Regional Government of Castilla y León (Junta de Castilla y León) and the Ministry of Science and Innovation MICIN and the European Union NextGenerationEU PRTR. Author Saul Vallejos received grant BG22/00086 funded by the Spanish Ministerio de Universidades. Author Marta Guembe-García received funding from the Spanish Ministerio de Universidades-European Union under the framework of NextGeneration EU RD 289/2021 for her Post-Doc position. We also acknowledge the financial support provided by MCIN/AEI/10.13039/501100011033 and by "ERDF A way of making Europe" (grant PID2020-113264RB-I00). Edurne González acknowledge the financial support of the Spanish Ministerio de Ciencia e Innovación (Proyectos de I+D+i, grant PID2020-117628RJ-I00). Issei Otsuka acknowledges the financial support of the French National Centre for Scientific Research (Emergence International grant).

*Supplementary Information*

Characterisation of the fluorogenic peptide substrate FITC-Ahx-FFK-Dabcyl. Additional characterisation of electrospun nanofibers. Growth curves of bacterial strains, *L. pneumophila* and *P. aeruginosa*. Sodium dodecyl sulfate polyacrylamide gel electrophoresis. Detection limits of smart materials for the detection of *L. pneumoniae*.

## Appendix A. Supporting information

Supplementary data associated with this article can be found in the online version at doi:10.1016/j.snb.2024.136976.

## Data availability

No data was used for the research described in the article.

## References

[1] M.A. Nisar, K.E. Ross, M.H. Brown, R. Bentham, J. Hinds, H. Whiley, Molecular screening and characterization of Legionella pneumophila associated free-living amoebae in domestic and hospital water systems, Water Res. 226 (2022) 119238, https://doi.org/10.1016/J.WATRES.2022.119238.
[2] World Health Organization, Chapter 11 - Laboratory aspects of Legionella, Legion. Prev. Legion. (2007).
[3] Z. Liu, Y.E. Lin, J.E. Stout, C.C. Hwang, R.D. Vidic, V.L. Yu, Effect of flow regimes on the presence of Legionella within the biofilm of a model plumbing system, J. Appl. Microbiol. 101 (2006) 437–442, https://doi.org/10.1111/J.1365-2672.2006.02970.X.
[4] Z. Chaabna, F. Forey, M. Reyrolle, S. Jarraud, D. Atlan, D. Fontvieille, C. Gilbert, Molecular diversity and high virulence of Legionella pneumophila strains isolated from biofilms developed within a warm spring of a thermal spa, BMC Microbiol. 13 (2013) 1–10, https://doi.org/10.1186/1471-2180-13-17/TABLES/3.
[5] A. Tata, F. Marzoli, M. Cordovana, A. Tiengo, C. Zacometti, A. Massaro, L. Barco, S. Belluco, R. Piro, A multi-center validation study on the discrimination of Legionella pneumophila sg.1, Legionella pneumophila sg. 2-15 and Legionella non-pneumophila isolates from water by FT-IR spectroscopy, Front. Microbiol. 14 (2023), https://doi.org/10.3389/fmicb.2023.1150942.
[6] M. Steinert, U. Hentschel, J.« Rg Hacker, Legionella pneumophila: an aquatic microbe goes astray, FEMS Microbiol. Rev. 26 (2002) 149–162, https://doi.org/10.1111/J.1574-6976.2002.TB00607.X.
[7] N. Miyashita, F. Higa, Y. Aoki, T. Kikuchi, M. Seki, K. Tateda, N. Maki, K. Uchino, K. Ogasawara, H. Kiyota, A. Watanabe, Distribution of Legionella species and serogroups in patients with culture-confirmed Legionella pneumonia, J. Infect. Chemother. 26 (2020) 411–417, https://doi.org/10.1016/J.JIAC.2019.12.016.
[8] A. Dey, Legionnaires' disease Annual Epidemiological Report for 2021 Key facts, (n.d.).

[9] O. Rossier, J. Dao, N.P. Cianciotto, The type II secretion system of Legionella pneumophila elaborates two aminopeptidases, as well as a metalloprotease that contributes to differential infection among protozoan hosts, Appl. Environ. Microbiol. 74 (2008) 753–761, https://doi.org/10.1128/AEM.01944-07/ASSET/25DD3423-E41A-44ED-B755-74FBD8574704/ASSETS/GRAPHIC/ZAM0030885450006.JPEG.
[10] J.N. Dowling, A.K. Saha, R.H. Glew, Virulence factors of the family Legionellaceae, Microbiol. Rev. 56 (1992) 32–60, https://doi.org/10.1128/MR.56.1.32-60.1992.
[11] L. Scheithauer, M.S. Karagöz, B.E. Mayer, M. Steinert, Protein sociology of ProA, Mip and other secreted virulence factors at the Legionella pneumophila surface, Front. Cell. Infect. Microbiol. 13 (2023) 1140688, https://doi.org/10.3389/FCIMB.2023.1140688/BIBTEX.
[12] N.P. Cianciotto, Many substrates and functions of type II secretion: lessons learned from Legionella pneumophila, Future Microbiol. 4 (2009) 797–805, https://doi.org/10.2217/FMB.09.53.
[13] E. Lammertyn, J. Anné, Protein secretion in Legionella pneumophila and its relation to virulence, FEMS Microbiol. Lett. 238 (2004) 273–279, https://doi.org/10.1016/J.FEMSLE.2004.07.056.
[14] L.A. Dreyfus, B.H. Iglewski, Purification and characterization of an extracellular protease of Legionella pneumophila, Infect. Immun. 51 (1986) 736–743, https://doi.org/10.1128/IAI.51.3.736-743.1986.
[15] J.S. Rosenfeld, F. Kueppers, T. Newkirk, R. Tamada, J.J. Meissler, T.K. Eisenstein, A protease from Legionella pneumophila with cytotoxic and dermal ulcerative activity, FEMS Microbiol. Lett. 37 (1986) 51–58, https://doi.org/10.1111/J.1574-6968.1986.TB01765.X.
[16] S.J. Blander, L. Szeto, H.A. Shuman, M.A. Horwitz, An immunoprotective molecule, the major secretory protein of Legionella pneumophila, is not a virulence factor in a guinea pig model of Legionnaires' disease, J. Clin. Invest. 86 (1990) 817–824, https://doi.org/10.1172/JCI114779.
[17] J.W. Conlan, A. Baskerville, L.A.E. Ashworth, Separation of Legionella pneumophila proteases and purification of a protease which produces lesions like those of Legionnaires' disease in guinea pig lung, J. Gen. Microbiol. 132 (1986) 1565–1574, https://doi.org/10.1099/00221287-132-6-1565.
[18] M.G. Keen, P.S. Hoffman, Characterization of a Legionella pneumophila extracellular protease exhibiting hemolytic and cytotoxic activities, Infect. Immun. 57 (1989) 732–738, https://doi.org/10.1128/IAI.57.3.732-738.1989.
[19] F.D. Quinn, L.S. Tompkins, Analysis of a cloned sequence of Legionella pneumophila encoding a 38 kD metalloprotease possessing haemolytic and cytotoxic activities, Mol. Microbiol. 3 (1989) 797–805, https://doi.org/10.1111/J.1365-2958.1989.TB00228.X.
[20] L. Szeto, H.A. Shuman, The Legionella pneumophila major secretory protein, a protease, is not required for intracellular growth or cell killing, Infect. Immun. 58 (1990) 2585–2592, https://doi.org/10.1128/IAI.58.8.2585-2592.1990.
[21] J.T. Walker, P.J. McDermott, Confirming the presence of Legionella pneumophila in your water system: a review of current legionella testing methods, J. AOAC Int. 104 (2021) 1135–1147, https://doi.org/10.1093/JAOACINT/QSAB003.
[22] K. Spies, S. Pleischl, B. Lange, B. Langer, I. Hübner, L. Jurzik, K. Luden, M. Exner, Comparison of the Legiolert™/Quanti-Tray® MPN test for the enumeration of Legionella pneumophila from potable water samples with the German regulatory requirements methods ISO 11731-2 and ISO 11731, Int. J. Hyg. Environ. Health 221 (2018) 1047–1053, https://doi.org/10.1016/J.IJHEH.2018.07.006.
[23] S.N. Monteiro, A.M. Robalo, R.J. Santos, Evaluation of Legiolert™ for the Detection of Legionella pneumophila and Comparison with Spread-Plate Culture and qPCR Methods, Curr. Microbiol. 78 (2021) 1792–1797, https://doi.org/10.1007/S00284-021-02436-6/TABLES/1.
[24] J.V. Lee, S. Lai, M. Exner, J. Lenz, V. Gaia, S. Casati, P. Hartemann, C. Lück, B. Pangon, M.L. Ricci, M. Scaturro, S. Fontana, M. Sabria, I. Sánchez, S. Assaf, S. Surman-Lee, An international trial of quantitative PCR for monitoring Legionella in artificial water systems, J. Appl. Microbiol. 110 (2011) 1032–1044, https://doi.org/10.1111/J.1365-2672.2011.04957.X.
[25] S. Collins, D. Stevenson, J. Walker, A. Bennett, Evaluation of Legionella real-time PCR against traditional culture for routine and public health testing of water samples, J. Appl. Microbiol. 122 (2017) 1692–1703, https://doi.org/10.1111/JAM.13461.
[26] S. Ahmed, U. Liwak-Muir, D. Walker, A. Zoldowski, A. Mears, S. Golovan, S. Mohr, P. Lem, C. Harder, Validation and in-field testing of a new on-site qPCR system for quantification of Legionella pneumophila according to ISO/TS 12869:2012 in HVAC cooling towers, J. Water Health 17 (2019) 237–253, https://doi.org/10.2166/WH.2019.252.
[27] P.L. Elverdal, C.S. Jørgensen, K.A. Krogfelt, S.A. Uldum, Two years' performance of an in-house ELISA for diagnosis of Legionnaires' disease: Detection of specific IgM and IgG antibodies against Legionella pneumophila serogroup 1, 3 and 6 in human serum, J. Microbiol. Methods 94 (2013) 94–97, https://doi.org/10.1016/J.MIMET.2013.04.010.
[28] A. Gholipour, M. Moosavian, M. Makvandi, H. Galehdari, A. Alvandi, S.A. Mard, Development of an indirect sandwich ELISA for detection of urinary antigen, using Legionella pneumophila PAL protein, World J. Microbiol. Biotechnol. 30 (2014) 1463–1471, https://doi.org/10.1007/S11274-013-1560-5/TABLES/3.
[29] J.C. Liao, M. Mastali, Y. Li, V. Gau, M.A. Suchard, J. Babbitt, J. Gornbein, E. M. Landaw, E.R.B. McCabe, B.M. Churchill, D.A. Haake, Development of an advanced electrochemical DNA biosensor for bacterial pathogen detection, J. Mol. Diagn. 9 (2007) 158–168, https://doi.org/10.2353/JMOLDX.2007.060052.
[30] J. Zhang, H. Yang, W. Liu, H. Wen, F. He, Rapid 16S rDNA electrochemical sensor for detection of bacteria based on the integration of target-triggered hairpin self-assembly and tripedal DNA walker amplification, Anal. Chim. Acta 1190 (2022) 339266, https://doi.org/10.1016/J.ACA.2021.339266.
[31] A. Laribi, S. Allegra, M. Souiri, R. Mzoughi, A. Othmane, F. Girardot, Legionella pneumophila sg1-sensing signal enhancement using a novel electrochemical immunosensor in dynamic detection mode, Talanta 215 (2020) 120904, https://doi.org/10.1016/J.TALANTA.2020.120904.
[32] E.J. Park, J.Y. Lee, J.H. Kim, C.J. Lee, H.S. Kim, N.K. Min, Investigation of plasma-functionalized multiwalled carbon nanotube film and its application of DNA sensor for Legionella pneumophila detection, Talanta 82 (2010) 904–911, https://doi.org/10.1016/J.TALANTA.2010.05.041.
[33] F. Mazur, A.D. Tjandra, Y. Zhou, Y. Gao, R. Chandrawati, Paper-based sensors for bacteria detection, Nat. Rev. Bioeng. 1 (2023) 180–192, https://doi.org/10.1038/s44222-023-00024-w.
[34] J. Zhang, M. Zhou, X. Li, Y. Fan, J. Li, K. Lu, H. Wen, J. Ren, Recent advances of fluorescent sensors for bacteria detection-a review, Talanta 254 (2023) 124133, https://doi.org/10.1016/J.TALANTA.2022.124133.
[35] D. He, Z. Wu, B. Cui, E. Xu, Z. Jin, Establishment of a dual mode immunochromatographic assay for Campylobacter jejuni detection, Food Chem. 289 (2019) 708–713, https://doi.org/10.1016/J.FOODCHEM.2019.03.106.
[36] F. Mazur, H. Tran, R.P. Kuchel, R. Chandrawati, Rapid detection of listeriolysin O toxin based on a nanoscale liposome-gold nanoparticle platform, ACS Appl. Nano Mater. 3 (2020) 7270–7280, https://doi.org/10.1021/acsanm.0c01602.
[37] S. Alhogail, R. Chinnappan, M. Alrifai, G.A.R.Y. Suaifan, F.J. Bikker, W.E. Kaman, K. Weber, D. Cialla-May, J. Popp, M.B. Alfageeh, K. Al-Kattan, M.M. Zourob, Simple and rapid peptide nanoprobe biosensor for the detection of: Legionellaceae, Analyst 146 (2021) 3568–3577, https://doi.org/10.1039/d1an00528f.
[38] M. Yang, X. Liu, Y. Luo, A.J. Pearlstein, S. Wang, H. Dillow, K. Reed, Z. Jia, A. Sharma, B. Zhou, D. Pearlstein, H. Yu, B. Zhang, Machine learning-enabled non-destructive paper chromogenic array detection of multiplexed viable pathogens on food, Nat. Food 2 (2021) 110–117, https://doi.org/10.1038/s43016-021-00229-5.
[39] G.A.R.Y. Suaifan, S. Alhogail, M. Zourob, Rapid and low-cost biosensor for the detection of Staphylococcus aureus, Biosens. Bioelectron. 90 (2017) 230–237, https://doi.org/10.1016/j.bios.2016.11.047.
[40] J.L. Vallejo-García, A. Arnaiz, M.D. Busto, J.M. García, S. Vallejos, Film-shaped reusable smart polymer to produce lactose-free milk by simple immersion, Eur. Polym. J. 200 (2023) 112495, https://doi.org/10.1016/J.EURPOLYMJ.2023.112495.
[41] A. Arnaiz, J.C. Guirado-Moreno, M. Guembe-García, R. Barros, J.A. Tamayo-Ramos, N. Fernández-Pampín, J.M. García, S. Vallejos, Lab-on-a-chip for the easy and visual detection of SARS-CoV-2 in saliva based on sensory polymers, Sens. Actuators B Chem. 379 (2023) 133165, https://doi.org/10.1016/J.SNB.2022.133165.
[42] V. Aragon, S. Kurtz, A. Flieger, B. Neumeister, N.P. Cianciotto, Secreted enzymatic activities of wild-type and pilD-deficient Legionella pneumophila, Infect. Immun. 68 (2000) 1855–1863, https://doi.org/10.1128/IAI.68.4.1855-1863.2000/ASSET/3F2F6889-BE6A-4B82-A49E-E990298B37A7/ASSETS/GRAPHIC/II0401578009.JPEG.
[43] R. Kapoor, R. Chawla, L.D.S. Yadav, Visible-light-mediated Gomberg-Bachmann reaction: an efficient photocatalytic approach to 2-aminobiphenyls, Tetrahedron Lett. 60 (2019) 805–809, https://doi.org/10.1016/J.TETLET.2019.02.022.
[44] D.M.P. De Oliveira, B.M. Forde, T.J. Kidd, P.N.A. Harris, M.A. Schembri, S. A. Beatson, D.L. Paterson, M.J. Walker, Antimicrobial resistance in ESKAPE pathogens, Clin. Microbiol. Rev. 33 (2020), https://doi.org/10.1128/CMR.00181-19/ASSET/3E4D6196-21E6-4155-9313-1CCEB9570E66/ASSETS/GRAPHIC/CMR.00181-19-F0001.JPEG.
[45] J. Denissen, B. Reyneke, M. Waso-Reyneke, B. Havenga, T. Barnard, S. Khan, W. Khan, Prevalence of ESKAPE pathogens in the environment: antibiotic resistance status, community-acquired infection and risk to human health, Int. J. Hyg. Environ. Health 244 (2022) 114006, https://doi.org/10.1016/J.IJHEH.2022.114006.
[46] A. Rani, V.B. Ravindran, A. Surapaneni, N. Mantri, A.S. Ball, Review: trends in point-of-care diagnosis for Escherichia coli O157:H7 in food and water, Int. J. Food Microbiol. 349 (2021) 109233, https://doi.org/10.1016/J.IJFOODMICRO.2021.109233.
[47] E.R. Green, J. Mecsas, Bacterial secretion systems – an overview, Microbiol. Spectr. 4 (2016), https://doi.org/10.1128/MICROBIOLSPEC.VMBF-0012-2015.
[48] E. Kessler, M. Safrin, J.C. Olson, D.E. Ohman, Secreted LasA of Pseudomonas aeruginosa is a staphylolytic protease, J. Biol. Chem. 268 (1993) 7503–7508, https://doi.org/10.1016/S0021-9258(18)53203-8.
[49] M.J. Everett, D.T. Davies, Pseudomonas aeruginosa elastase (LasB) as a therapeutic target, Drug Discov. Today 26 (2021) 2108–2123, https://doi.org/10.1016/J.DRUDIS.2021.02.026.
[50] M. Andrejko, A. Siemińska-Kuczer, M. Janczarek, E. Janik, M. Bednarczyk, M. Gagoś, M. Cytryńska, Pseudomonas aeruginosa alkaline protease exhibits a high renaturation capability, Acta Biochim. Pol. 66 (2019) 91–100, https://doi.org/10.18388/ABP.2018_2741.
[51] A.J. Saleem, A.J. Saleem, Relationship study between the alkaline protease production and the growth phases of Pseudomonas aeruginosa isolated from patients, Adv. Microbiol. 2 (2012) 354–357, https://doi.org/10.4236/AIM.2012.23043.

**Dr. Ana Arnaiz** (F) completed her PhD in Biotechnology and Genetic Resources in Plants and Associated Microorganisms at the Universidad Politécnica de Madrid in 2019. She also received a postdoctoral Margarita Salas Grant at the University of Burgos to expand her research in smart polymeric materials. She currently holds a postdoctoral fellowship at the University of Burgos and is focused on the development of sensory polymeric materials oriented towards detecting biological targets.

**Dr. Marta Guembe-García** (F) received her PhD in Advanced Chemistry from the University of Burgos, Spain, in 2021. In 2022, she was awarded a two-year postdoctoral Margarita Salas Grant at the University of Pavia, Italy, to further her research in the development of smart materials for various analytical chemistry applications. She is currently working at the University of Burgos. Her research focuses on smart polymeric materials for advanced applications, including sensory polymers and high-performance materials.

**Mario Martinez** (M) graduated in chemistry from the University of the Basque Country (UPV/EHU) in July 2021. He completed the final degree project in the catalysis group under the supervision of Prof. Oihane Sanz Iturralde. During the summer of 2021, he did an internship in the same catalysis group. During the 2021–2022 period, Mario completed a double Master's degree in Chemistry and Polymers at the University of the Basque Country (UPV/EHU) and the Université de Bordeaux, specializing in polymers. During the masterś thesis project, Mario studied the synthesis of functional hybrid nanofibers under the supervision of Dr. Edurne González and Prof. Oihane Sanz Iturralde. His current research is focused on the obtention of functional nanometer scale fibers by electrospinning technique.

**Miriam Trigo-López** (F) received her Ph.D. in Advanced Chemistry from the University of Burgos, Spain, in 2015. She is currently a research staff member in the Department of Chemistry at the same university. Her research focuses on functional polymers for advanced applications, including sensory polymers and high-performance materials.

**Dr. Edurne Gonzalez** (F) obtained her phD in 2013 from the University of the Basque Country (UPV/EHU). After a post-doctoral research experience at Cornell University (USA) and the Materials Physics Center (Spain), she is currently an Assistant Professor in Chemical Engineering at the Chemistry Faculty of UPV/EHU. Her research is focussed on two main lines; the development of sustainable waterborne polymer dispersions and the fabrication of advanced functional nanofibers by Green-Electrospinning process

**Dr. Issei Otsuka** (M) is a permanent researcher of the French National Centre for Scientific Research (CNRS) at CERMAV. He received his PhD in Macromolecular Chemistry from Hokkaido University, Japan in 2008. He received his Research Habilitation Degree (HDR) in 2019 from the University of Grenoble Alpes, France. Dr. Otsuka is the author/co-author of 60+ peer-reviewed scientific publications, patents, and book chapters. His recent research activity focuses on structuring functional polysaccharide derivatives by electrospinning toward various biomedical applications.

**Dr. Saúl Vallejos** (M) received his PhD in Chemistry in 2014 from the University of Burgos, Spain. Now, he is the Lab Head of the POLYMERS RESEARCH GROUP at the Department of Chemistry, University of Burgos. Dr. Vallejos is the author/co-author of 60+ peer-reviewed scientific publications, 23 patents, and co-author of books and book chapters. His research interests are functional polymers with receptor motifs as sensory materials for anions, cations, and neutral molecules.